Journal Name

ARTICLE

α-Fluoro-*o*-cresols: the key role of intramolecular hydrogen bond in conformational preferences and hydrogen-bond acidity.

Received 00th January 20xx,
Accepted 00th January 20xx

DOI: 10.1039/x0xx00000x

www.rsc.org/

E. Bogdan,[a,*] A. Quarré de Verneuil,[a] F. Besseau,[a] G. Compain,[b] B. Linclau,[b] J.-Y. Le Questel[a] and J. Graton[a,*]

The conformational preferences of *o*-cresols driven by fluorination have been thoroughly investigated from a theoretical point of view with quantum chemical methods and compared to those recently reported for benzyl alcohols. Key conformers of both families exhibit a 6-membered intramolecular hydrogen-bond (IMHB) interaction. A significant enhancement of IMHB strength is observed in α-fluoro-*o*-cresols, owing to the simultaneous increase of the aliphatic fluorine hydrogen-bond (HB) basicity and of the aromatic hydroxyl HB acidity, compared to *o*-fluorobenzyl alcohols, which are characterized by aromatic fluorine atoms and aliphatic hydroxyl groups. In the case of di- and trifluorinated derivatives, the occurrence of a three-centre hydrogen-bond is emphasised and its features discussed. The impact of these structural predilections on *o*-cresol HB properties has been characterised from the estimation of the HB acidity parameter, pK_{AHY}, weighted according to their conformational populations. We find that α-fluorination leads to an HB acidity decrease of the hydroxyl group (in contrast with *o*-fluorination of benzyl alcohols), whereas α,α-difluorination results in no significant variation of pK_{AHY}. Finally, an increase of HB acidity is predicted upon methyl perfluorination, which has been confirmed experimentally. Theoretical descriptors based on AIM, NCI and NBO analyses allows rationalizing the predicted trends, and reveal a relationship with the strength of the established OH···F IMHB.

Introduction

The effects of fluorination on molecular properties are well established, and their use in compound property optimisation in many fields like material[1, 2] and medicinal chemistry,[3-6] as well as crystal engineering[7, 8] and agrochemistry[9, 10] benefit from this strong influence. After the debate about the effective ability of fluorine to act as a hydrogen-bond (H-bond, HB) acceptor,[11-15] the occurrence of intermolecular OH···F H-bonding is now clearly established through experimental and theoretical evidences.[16-20] The existence of intramolecular hydrogen bonds (IMHBs) involving fluorine has also been scrutinised and highlighted experimentally through NMR techniques for conformationally constrained,[21-23] partially flexible,[24] and even fully flexible fluorohydrins.[25] We have recently reported that the intermolecular hydroxyl H-bond donating capacity (or HB acidity) in conformationally fixed fluorohydrins (eg **1**, Figure 1)[21] and partially flexible benzyl alcohols (eg **2**)[26] is deeply influenced by the conformational preferences dictated by the presence of such IMHBs. Thus, the H-bond acidity of **1** was significantly decreased, and attributed to a rather strong IMHB (6-membered ring motif). On the contrary, in *o*-fluorobenzyl alcohols such as **2a**,**b** where a similar 6-membered IMHB interaction is possible, we observed an *increase* of H-bond donating capacity upon a first fluorination, followed by a *decrease* upon a second fluorination: all *o*,*o'*-difluorobenzyl alcohols investigated were systematically worse H-bond donors than their non-fluorinated parent. These trends were rationalised by showing that the corresponding OH···F IMHB is not only much weaker, but also of secondary importance with respect to the conformational constraint imposed by the *ortho* fluorine atoms. With fluorobenzyl alcohols, the IMHB involves an aromatic fluorine (sp^2 C–F) and an aliphatic hydroxyl group, and it is indeed of interest to compare this type of motif to α-fluoro-*o*-cresol derivatives **3** (sp^3 C–F, Figure 1), bearing an aliphatic fluorine and an aromatic hydroxyl group.

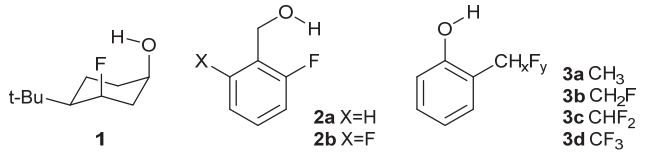

Figure 1. Structures of compounds previously investigated (**1** and **2a**, **2b**) and of *o*-cresols (**3a**-**3d**) studied in the present work.

Thus, the aim of this work is to compare the properties of α-fluoro-*o*-cresol derivatives with these of the previously reported fluorinated benzyl alcohols, since the aliphatic fluorine atom is

[a] *CEISAM UMR CNRS 6230, Faculté des Sciences et des Techniques, Université de Nantes 2, rue de la Houssinière BP 92208, 44322 NANTES Cedex 3 (France) Fax: (+3) 2-51-12-54-02, E-mail : elena.bogdan@univ-nantes.fr ; jerome.graton@univ-nantes.fr.*
[b] *Chemistry, University of Southampton, Highfield, Southampton SO17 1BJ (UK).*
† Footnotes relating to the title and/or authors should appear here.
Electronic Supplementary Information (ESI) available: [details of any supplementary information available should be included here]. See DOI: 10.1039/x0xx00000x

expected to show an enhanced HB accepting ability[19] and the aromatic hydroxyl group an enhanced HB donating capacity, compared to the situation in the benzyl alcohols.[27, 28]

Hence, the conformational landscapes and the H-bond acidity properties of *o*-cresols with various degrees of fluorination (**3a–d**) are explored and quantified through density functional theory (DFT) calculations. Topological (Atoms in Molecules (AIM),[29, 30] Non Covalent Interactions (NCI)[31] and Natural Bond Orbital (NBO)[32]) analyses were carried out to compare IMHB interactions occurring in fluorinated *o*-cresols **3** and the benzyl alcohols **2**.

The H-bond acidity, pK_{AHY}, was measured experimentally for available compounds, and systematically evaluated with the computation of the electrostatic potential descriptor, $V_\alpha(r)$.[33]

Experimental section

Computational details

All DFT calculations were performed using the D.01 version of the Gaussian 09 program.[34] A conformational analysis of *o*-cresols and phenols derivatives were performed at the MPWB1K/6-31+G(d,p) level of theory in CCl_4. The vibrational spectrum was computed for each optimized structure in order to check that a true minimum was found on the basis of its harmonic vibrational frequencies and to calculate the Gibbs free energy *G* of the corresponding conformer. Solvent effects were included using the polarizable continuum model within the integral equation formalism (IEF-PCM). The relative populations p_i (Eq. [1]) of the various conformers were hence evaluated through a Boltzmann distribution from the corresponding computed Gibbs free energy differences (ΔG_i) .

$$p_i = \frac{e^{-\Delta G_i/RT}}{\sum_{i=1}^{n} e^{-\Delta G_i/RT}} \qquad [1]$$

The various theoretical descriptors calculated in a second step were weighted according to these computed populations.

With the aim to gain more insights on the IMHB interactions occurring in the relevant conformers, AIM topological analyses[29, 30] of the IEF-PCM/MP2/6-311++G(2d,p) wave functions were thoroughly carried out using the AIM2000 program.[35] Besides the electron densities ρ_{bcp} and their Laplacians $\nabla^2\rho_{bcp}$, the potential energy density V_{bcp} at the bond critical point (bcp) has previously been shown to bring additional relevant information, in particular on the strength of a given HB.[36-38] Thus, HB energies (E_{HB}) estimated from the potential energy densities V_{bcp} according to the established relationship in Equation [2],[39] have also been computed in the present study.

$$E_{HB} = \tfrac{1}{2} |V_{bcp}| \qquad [2]$$

In addition, Non-Covalent Interaction (NCI)[31] analyses of the same wavefunctions were performed using the NCIPLOT 3.0 program,[40] specifically in cases where the AIM procedure failed to detect bcp.

Finally, the charge transfer between the acceptor lone pair and the σ* donor antibonding orbital has been investigated through Natural Bond Orbital (NBO) analyses.[32] The NBO method has been applied at the IEF-PCM/MPWB1K/6-31+G(d,p) level to provide the corresponding interaction energies $E^{(2)}_{n\rightarrow\sigma^*}$ evaluated from the second-order perturbation theory.

Key NBO descriptors relevant for the present study, in particular, the occupancies of the molecular orbitals involved (fluorine lone pairs and σ^*_{OH}) have also been examined in detail.

The HB acidity of the compounds under study were evaluated as recommended by Kenny through the $V_\alpha(r)$ descriptor,[33] calculated along the OH bond at a distance r = 0.55 Å from the hydroxyl hydrogen atom. This parameter was calculated using the MPWB1K/6-31+G(d,p) wavefunctions in vacuo, as computed previously for the established calibration line (Equation [3]).

$$pK_{AHY} = 52.16\, V_\alpha(r) - 15.94 \qquad [3]$$
$$n=43,\ r^2 = 0.9812,\ s = 0.11,\ F = 2142$$

Chemicals.

The commercially available compounds **3a** and **3d** were purified by standard procedures and carefully dried over 4 Å molecular sieves. Spectroscopic grade carbon tetrachloride was kept for several days over freshly activated 4 Å molecular sieves before use. Commercial *N*-methyl-2-pyrrolidinone (>99.5% purity) was also stored over molecular sieves in the dark.

FTIR spectrometry measurements.

The handling of all chemicals, of their CCl_4 solutions and the filling of the cells for IR measurements were performed in dry glove box atmosphere at room temperature. IR spectra were recorded in carbon tetrachloride solutions with a Fourier transform spectrometer (Bruker Vertex 70) at a resolution of 1 cm^{-1}. An Infrasil quartz cell (ℓ=1cm path length and thermostatted at 25.0±0.2°C by Peltier effect regulation) was used for the studies of HB complexation. The HB donating capacities or HB acidities (pK_{AHY} values) of the cyclic alcohols were determined by using the IR method through complexation with a standard HB acceptor, N-methyl-2-pyrrolidinone (NMP) in CCl_4 at 25°C (Scheme 1).

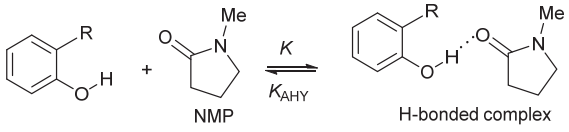

$$pK_{AHY} = -\log_{10}K_{AHY} = +\log_{10}K$$

Scheme 1. Experimental determination of *o*-substituted phenols HB acidity.

The molar absorption coefficients, ε_{OH}, required for the equilibrium constant measurements, were determined for each compound at the free OH stretching frequency (ν_{OH}) of the absorption maxima.

Results and discussion

Conformational preferences of α-fluoro-*o*-cresols.

Within the *o*-halophenol series, two conformers with the O–H bond in the plane of the aryl ring can be distinguished, and are usually identified as the *cis* and *trans* conformations. For α-fluoro-*o*-cresols, the additional degree of freedom induced by

the fluoromethyl group requires a second descriptor. In this regard, the nomenclature as previously defined for the description of the benzyl alcohol conformations is particularly relevant.[26] For the OH conformation, *proximal* (*P*) and *distal* (*D*) conformers are defined (Figure 2), next to a *gauche* (*G*) conformation. For the methyl group, one atom is typically located in the plane of the aromatic ring (and *distal* towards the hydroxyl substituent). With monofluorination, the C–F bond is either in the *plane* (*pl*) of the aromatic ring, or in a *gauche* (*g*) conformation (Figure 2). In a few cases, a perpendicular conformation (*perp*) is also observed. With difluoromethylation, the same conformations can be distinguished but now related to the C-H bond.

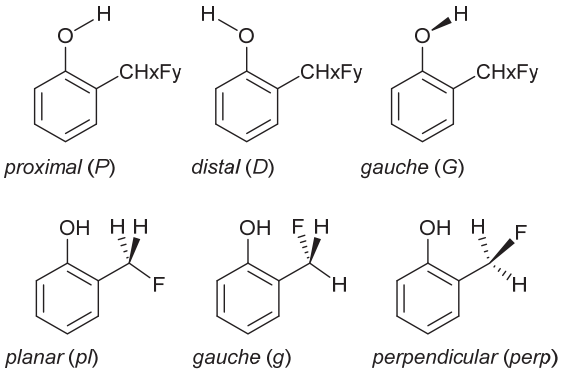

Figure 2. Selected nomenclature describing the *o*-cresols conformations.

The conformational analysis of the cresol derivatives (Table 1) shows that the degree of fluorination significantly impacts on the preferred conformations of *o*-cresols. In most cases, OH···F IMHB conformers are observed, which are characterised by the following structural features: $d_{OH\cdots F}$, the intramolecular HB length, $\theta_{OH\cdots F}$ the valence angle assessing the linearity of the interaction, and φ_{CCOH} and $\varphi_{COH\cdots F}$ dihedral angles that allow measuring its directionality. More precisely, the first (φ_{CCOH}) quantifies the deviation of the OH bond from the aromatic plane whereas the latter ($\varphi_{COH\cdots F}$) describes the position of the OH bond towards the fluorine atom. The stabilised conformations are shown in Figure 3.

In *o*-cresol **3a**, two different conformers are found with a predilection for conformation ***D*** explained by a destabilization of the ***P*** form by repulsion of the methyl (C-H) and hydroxyl (O-H) groups (Figure 3).

The most populated conformation (60%) of **3b**, ***G/g***, shows an OH···F IMHB, with a slight deviation of the OH group (φ_{CCOH} = 21°) resulting in a *gauche* rather than a *proximal* conformation and optimising the OH group orientation towards the fluorine atom ($\varphi_{COH\cdots F}$ = -3°). This relaxation leads to a short OH···F distance of 1.98Å suggesting an optimal IMHB interaction. In the gas phase, this OH···F distance had been estimated to be shorter (1.88Å), at the B3LYP/6-31G(d,p) level of theory.[41] Within our methodology of calculation, we also have identified two other conformations, named ***D/pl*** and ***D/perp***, with computed populations of 28% and 12%, respectively.

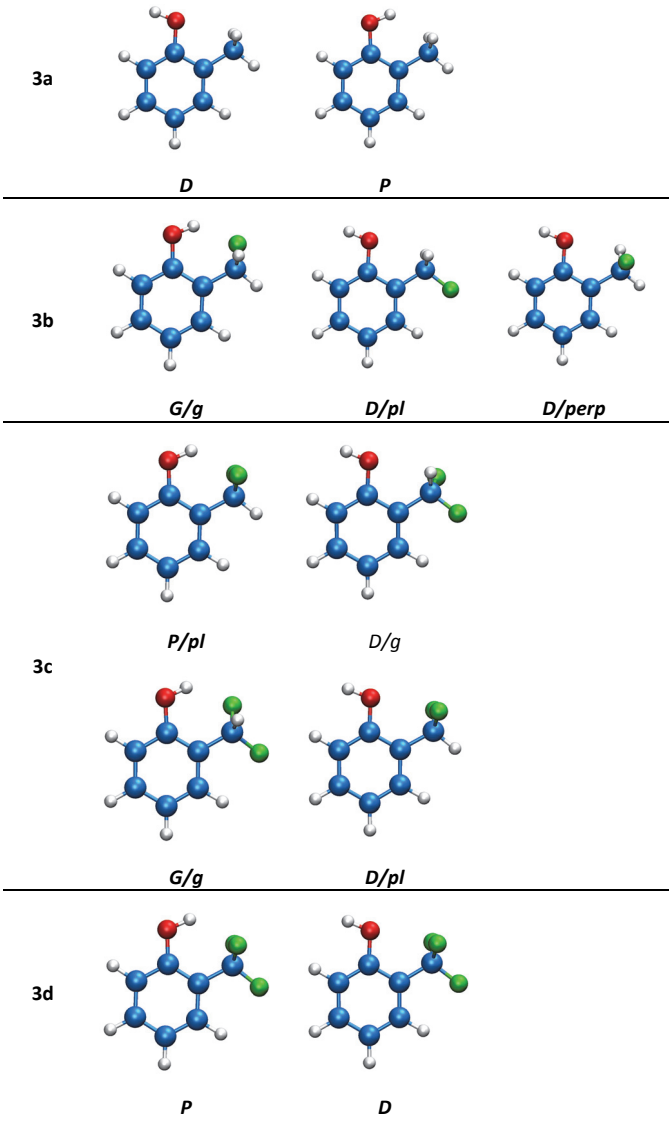

Figure 3. Stabilised conformations identified for the o-cresols **3a–3d** in CCl_4 (IEF-PCM/MPWB1K/6-31+G(d,p)).

The α,α-difluoro-*o*-cresol **3c**, shows two stabilised conformations with an OH···F interaction. In comparison with **3b *G/g***, the population of the **3c *G/g*** conformer is reduced to 14%, and is subjected to a slight lengthening of the OH···F distance (1.99Å), the OH group being located 23° out of the plane, oriented towards the fluorine atom ($\varphi_{COH\cdots F}$ = -7°). The preferred conformer (50%, ***P/pl***) actually corresponds to a three-centre IMHB structure (Figure 3) with two longer OH···F distances (2.27Å, still significantly shorter than the sum of the van der Waals radii[42]), and a significantly narrower $\theta_{OH\cdots F}$ angle (123° instead of 138°). Two other conformations with a *distal* orientation of the hydroxyl group are found, ***D/g*** and ***D/pl***, with estimated populations of 34% and 2%, respectively. Conversely, in the gas phase at the B3LYP/6-31+G(d,p) level, the ***P/pl*** conformer had previously been attributed to a transition state structure.[43] Furthermore, in the same work a ***G/pl*** form was obtained as the absolute energetic minimum, showing only a

two-centre IMHB,[43] whereas it does not appear as a stationary point through our calculations.

Finally, similarly to *o*-cresol, α,α,α-trifluoro-*o*-cresol **3d** is found only in ***P*** and ***D*** conformations, the *proximal* form being significantly favoured (79%) thanks to a three-centre IMHB with two of the three fluorine atoms (2.22 and 2.38 Å). Contrary to the **3c** ***P/pl*** conformer, the OH bond slightly deviates from the aromatic ring plane (φ_{CCOH} = 4.4°), and the HB linearity ($\theta_{OH\cdots F}$ = 125.6; 118.5°) and directionality ($\varphi_{COH\cdots F}$ = 27.1; -38.6°) are non-equivalent for each fluorine atom. This bifurcated IMHB conformation has been attributed in a previous work as the structure of **3d** by gas-phase electron diffraction[44] and microwave spectroscopy,[45] even if a real consensus was not found, neither on its preferred conformation,[41, 43, 46] nor on the nature of hydrogen-bond of the corresponding intramolecular OH···F interaction.[47] In our calculations, the three-centre IMHB involving two fluorine atoms with two identical OH···F distances was identified as a transition state for **3d**. This result is in line with the computational study of Knak Jensen *et al* (B3LYP/6-31+G(d,p) level),[43] although their identified minimum energy structures included only one OH···F IMHB.

Table 1. Calculated Gibbs free energy differences and relative populations of the main o-cresols conformers with the corresponding optimized geometrical features in CCl_4 medium.

Conformer		ΔG [a], kJ·mol^{-1}	p_i [a], %	$d_{OH\cdots F}$ [b], Å	$\theta_{OH\cdots F}$ [b], °	φ_{CCOH} [b], °	$\varphi_{COH\cdots F}$ [b], °	φ_{CCCX} [b], °
3a	*D*	0.0	73			180.0		180.0 [c]
	P	2.4	27			0.0		180.0 [c]
3b	*G/g*	0.0	60	1.982	138.0	21.3	-3.1	-52.9 [d]
	D/pl	0.1	28			179.6		180.0 [d]
	D/perp	4.0	12			180.0		81.0 [d]
3c	*P/pl*	0.0	50	2.267; 2.267	123.4; 123.4	0.0	34.8; -34.8	180.0 [c]
	D/g	2.6	34			178.9		42.2 [c]
	G/g	4.9	14	1.993	135.3	23.0	-7.4	68.5 [c]
	D/pl	9.2	2			179.7		177.9 [c]
3d	*P*	0.0	79	2.224; 2.379	125.6; 118.5	4.4	27.1; -38.6	177.9 [d]
	D	1.6	21			180.0		180.0 [d]

[a] Calculated at IEF-PCM/MPWB1K/6-31+G(d,p) level of theory, with the most stable structure of each compound taken as reference. [b] Optimized, distances, valence angles and dihedral angles calculated at the MPWB1K/6-31+G(d,p) level of theory in CCl_4. [c] X=H. [d] X=F.

Hence, in CCl_4 medium, our theoretical results show that the most stable and most populated conformers for all fluorinated *o*-cresols (**3b** – **3d**) involve a 6-membered IMHB interaction. In our recent work focusing on *o*-fluorinated benzyl alcohols,[26] we have shown that such 6-membered OH···F IMHB structures were also stabilised conformers, as illustrated in Figure 4. But, in contrast to α-fluoro-*o*-cresol, they were not necessary the most stable conformers. Instead, they only appeared as the most populated conformations when the structure was bearing two *o*-fluorine substituents (**2b**).

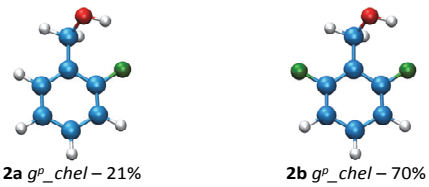

2a g^p*_chel* – 21% **2b** g^p*_chel* – 70%

Figure 4. Stabilised g^p*_chel* conformers of *o*-fluorobenzyl alcohols **2a** and **2b** investigated previously,[26] together with their relative population.

AIM, NCI and NBO analyses.

For a better understanding of the relation between the degree of fluorination of the various compounds and their conformational preferences, we have carried out a number of wavefunction analyses.

At first, AIM analyses was applied to identify and characterise IMHB interactions. A bond critical point was systematically detected in conformations with an IM interaction forming a 6-membered ring (Figure 5). The electron densities calculated at these critical points reach 0.021 e bohr^{-3}, a typical value for a H-bond interaction,[48, 49] for the ***G/g*** conformers of **3b** and **3c**, respectively. These values are very close to those found by Shapiro *et al.*[50] in the case of 2,6-bis(fluoromethyl)phenol. Very interestingly, in the ***P/pl*** conformation of **3c**, this electron density is shared symmetrically (0.013 e bohr^{-3}) between the two fluorine atoms validating the HB motif as a three-centre interaction. However, in the ***P*** conformation of **3d,** only one bcp was found, for the shortest OH···F distance.

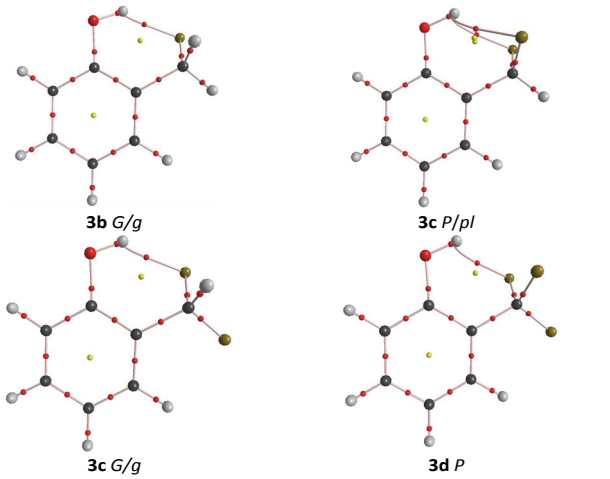

Figure 5. QTAIM molecular graphs for the chelated conformers of fluorinated cresols **3b-3d**.

Based on the potential energy density, V_{bcp}, calculated at the bcp, E_{HB} can provide an estimation of the relative strength of the IMHB interactions for these *o*-fluorocresols (Table 2), that can also be compared with previously studied benzylalcohols,[26] the same level of theory being selected. In agreement with the shortest OH···F distances, the highest estimated HB energies (around 25 kJ mol^{-1}) are found for the ***G/g*** conformations of compounds **3b** and **3c**, respectively. Weaker individual HB energies (around 15 kJ mol^{-1}) are observed for the three-centre structures, but overall, the cooperativity between both interactions (as shown in the case of **3c**) yields to a higher stabilization of this conformation. The electron density and the HB energy values suggest that the IMHBs occurring in *o*-fluorocresols are significantly stronger than in *o*-fluorobenzyl alcohols[26] for the two–centre OH···F interactions, and of the same order of magnitude for the three-centre OH···F interactions.

Secondly, a complementary NCI analysis was carried out for all conformers identified for compounds **3b**-**3d**. Thus, the electron density and its derivative, reduced density gradient (RDG), were computed and compared (plots of the RDG *versus* sign$\lambda_2(\rho)$ and RDG isosurfaces in the ESI). For **3b *G/g***, **3c *G/g*** and **3c *P/pl***, the plots show an attractive OH···F interaction. For the latter two areas with equivalent attractive interactions between the hydroxyl group and the fluorine atoms are observed (Figure 6) attesting the presence of a three-centre IMHB interaction in in **3c**, as found through our AIM analysis. Interestingly, such a three-centre IMHB is also found for conformer **3d *P***, but with two non-equivalent HB interactions in this case, as revealed by the geometrical data. The other conformers (reported in the ESI) show in some situations additional attractive contributions between the fluorine and the ortho CH bond when the CF bond is planar with respect to the aromatic ring, with electron densities around 0.010 a.u. (see **3b *D/pl***, **3c *D/g***, **3c *G/g***, **3d *P*** and **3d *D***). Finally, no clear trends can be established for the H···H, O···F and O···H interactions, the sign of λ_2, and hence the attractive or repulsive character of the interaction, depending significantly on the method of calculation in very weak interactions.[51]

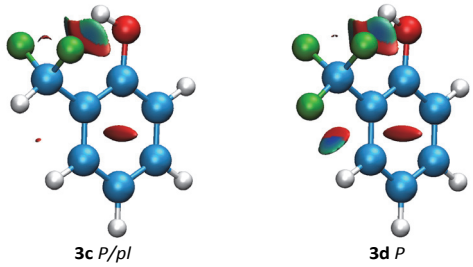

Figure 6. NCI isosurface plots drawn with a reduced density gradient (RDG) value of 0.6 and blue-green-red values ranging from -0.02 to 0.01 a.u for the three-centre IMHB conformations of **3c** and **3d**. Large, negative values of sign(λ_2)ρ (blue colour) are indicative of attractive interactions (such as dipole – dipole or HB interactions); while if sign(λ_2)ρ is large and positive (red colour) they are indicative of repulsive forces. Nonbonding or very weak interactions, such as van der Waals interactions, show values near zero that are coloured in green.

Table 2. AIM and NBO computed descriptors of the IMHB conformers of studied α-fluoro-*o*-cresols.

Conformer	ρ_{bcp} [a] e·bohr^{-3}	$\nabla^2\rho$ [a]	E_{HB} [a] kJ·mol^{-1}	$E^{(2)}_{n\rightarrow\sigma^*}$ [b] kJ·mol^{-1}
3b *G/g*	0.0211	0.0881	25.3	3.6 / – / 22.6
3c *P/pl*	0.0128	0.0564	14.6	0.9 / 2.7 / 2.3
	0.0128	0.0564	14.6	0.9 / 2.7 / 2.3
3c *G/g*	0.0211	0.0871	24.8	5.0 / – / 19.2
3d *P*	0.0137	0.0585	15.4	1.2 / 5.3 / -
	0.0131 [c]			- / - / 2.2

[a] AIM electron density and its gradient value at the bond critical point and HB energy at the IEF-PCM/MP2/6-311++G(2d,p) level. [b] Charge transfer energies from the three n_F fluorine lone pairs to the σ^*_{OH} antibonding orbital at the MPWB1K/6-31+G(d,p) level. [c] electron density value provided by the NCI analysis since the AIM procedure does not detect any bcp.

Finally, within the NBO procedure, the OH···F IMHB interactions were investigated by calculation of charge transfer energies ($E^{(2)}_{n\rightarrow\sigma^*}$) between the fluorine lone pair and the sigma antibonding OH orbital, complemented by calculations of the corresponding orbital occupancies (Tables 2 and SI1). The $E^{(2)}_{n\rightarrow\sigma^*}$ values calculated for the two-centre IMHB conformations (from 19 to 23 kJ mol^{-1}) confirm that they are much stronger than in *o*-fluorobenzyl alcohols (4.6 and 4.4 kJ mol^{-1} in **2a** and **2b**, respectively).[26] For the three-centre IMHB conformations, the corresponding energy is calculated to be much weaker, with two equivalent contributions from the two fluorine atoms involved in **3c**. Conversely, in **3d**, the $E^{(2)}_{n\rightarrow\sigma^*}$ energies are different owing to the non-equivalence of the two OH···F IMHBs. Interestingly, the computed occupancy of the σ^*_{OH} antibonding orbital increases from the conformers without any IMHB interaction (ca. 0.008 e) to those showing a two-centre IMHB (ca. 0.016 e), an intermediate value (ca. 0.012 e) being found in three-centre IMHB structures. Unexpectedly, the concomitant decrease of the fluorine lone pairs occupancy was not observed. The relative contributions of the various atomic orbitals constituting the natural bond orbitals involved in the IMHB interaction do not change significantly from one compound to another (**3b** *versus* **3c** and **3d**) and from one conformation to another (2-centre *versus* 3-centre). The most involved fluorine lone pairs are 100% p atomic orbitals of

fluorine, and the OH antibonding orbital is constituted by 23% of a sp^3 hybrid orbital of oxygen and 77% of the s atomic orbital of hydrogen.

Other relevant conformational features can be pointed out from NBO calculations. Hence, strong charge transfer energies from 30 to 45 kJ mol^{-1} (see the ESI) are computed between the $\pi_{C=C}$ bonding orbital and the σ^*_{CF} antibonding orbital when the CF bond is gauche, or even better perpendicular, to the aromatic ring. In these cases, an increase of around 0.020 e is observed within the σ^*_{CF} antibonding orbital.

Estimation of α-fluoro-*o*-cresols HB-acidity.

The a significant proportion of IMHB conformers in all the α-fluoro-o-cresols studied are expected to influence the HB properties of the hydroxyl group of the fluorinated derivatives. In this section, the HB donating capacity (pK_{AHY}) of relevant compounds has therefore been investigated to quantify these effects.

Experimental measurement of the cresol H-bond acidities was only possible for compounds **3a** and **3d**, given the known instability of α-fluoro and α,α-difluoro-*o*-cresols.[52, 53] In the case of *o*-cresol **3a**, the presence of the methyl group, an electrondonating substituent, slightly decreases the hydroxyl H-bond donating capacity in comparison with phenol (pK_{AHY} = 1.92 and 2.06,[27] respectively). On the contrary, the strong electronwithdrawing effect of the CF_3 substituent yields to an expected strong increase of H-bond acidity (pK_{AHY} = 2.59).

In recent studies, we have confirmed the interest of $V_\alpha(r)$, initially introduced by Kenny,[33] to appropriately estimate the HB acidity of hydroxyl compounds,[27] as well as to take into account the fluorine influence on this property.[21, 26] We have therefore calculated $V_\alpha(r)$ for the current series of cresol derivatives. The conformational analysis carried out above allows us to calculate weighted values of $V_\alpha(r)$, reported in Table 3 with the estimated pK_{AHY} values, and illustrated in Figure 7. Hence, *o*-cresol **3a** exhibits a H-bond acidity value (pK_{AHY} = 2.11) typical of that encountered for a phenol derivative. Upon a first fluorination in **3b**, a strong decrease of H-bond acidity (ΔpK = -0.55) is predicted. While the electronwithdrawing effect of fluorine could be expected to result in an increased H-bond acidity, the IMHB interaction results in a decreased propensity of the OH group to interact with an intermolecular H-bond acceptor. The introduction of a second fluorine atom (**3c**) allows recovering the initial H-bond acidity of non-fluorinated *o*-cresol (pK_{AHY} = 2.11). Finally the electronwithdrawing effect of the trifluoromethyl group is strong enough to induce a significant pK_{AHY} increase (**3d**), as observed experimentally.

Table 3. $V_\alpha(r)$ electrostatic potential values used for the estimation of the HB acidity of the cresol series.

Compound	$\bar{V}_\alpha(r)$ [a]	$pK_{AHY(calc)}$ [b]	$pK_{AHY(exp)}$
3a	0.3461	2.11	1.92
3b	0.3355	1.56	n.d.
3c	0.3460	2.11	n.d.
3d	0.3524	2.44	2.59

[a] values weighted by the conformational populations in CCl_4 medium at the MPWB1K/6-31+G(d,p) level. [b] estimated with Eq. (3).

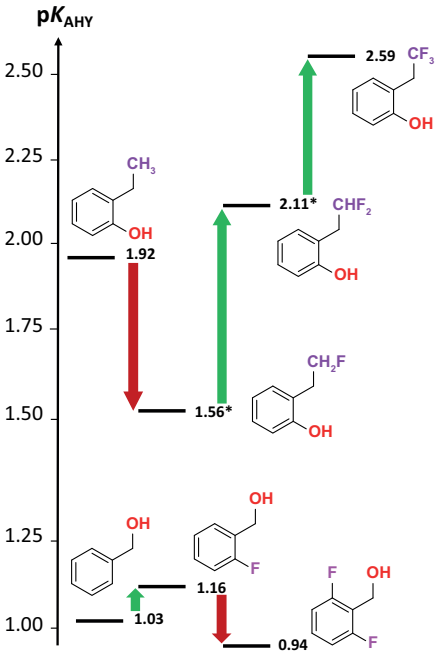

Figure 7. H-bond acidity evolution of *o*-cresols upon increasing degrees of fluorination of the methyl group. The starred values are computed ones.The experimental variation observed with *o*-fluorobenzyl alcohols is given for comparison.

Despite the structural similarities of *o*-cresols and *o*-benzyl alcohols, with both allowing for the occurrence of a 6-membered IMHB interaction, our results show strongly distinct behaviours regarding their H-bond acidity evolution upon fluorination (Figure 7). These trends are clearly rationalised considering the features of the established IMHB highlighted above. In the *o*-fluorocresol series (**3b**-**3d**), the IMHB distances were determined as significantly shorter and energetically much stronger, as illustrated by the AIM and NBO analyses, compared to the equivalent IMHB in the *o*-fluoro benzyl alcohols. Hence, whereas *ortho*-monofluorination of benzyl alcohol induces a H-bond acidity increase, α-monofluorination of *o*-cresol leads to a decrease in H-bond acidity compared to their non-fluorinated 'parents'. On the contrary, *o*,*o*-difluorination of benzyl alcohol leads to a decrease in H-bond acidity, while an increase is predicted upon α,α-difluorination of *o*-cresol.

Conclusions

This work provides new experimental and theoretical evidences of the peculiar and significant influence of fluorination on molecular properties of hydroxyl groups in different chemical environments. For a series of *o*-cresols of increasing degree of fluorination, we show that the presence of the fluorine atom on the methyl group favours the chelated conformations in which an intramolecular interaction occurs between the hydroxyl and the fluorine moieties. The features of this interaction (intramolecular distances, electron densities calculated at the bcp, charge transfer values) clearly indicate that it corresponds to an OH···F IMHB. The various parameters show that the IMHB interaction strength is much higher in α-fluoro-*o*-cresols than in the case of *o*-fluorobenzyl alcohols. Consequently, in contrast to the situation in *o*-fluorobenzyl alcohols, the intramolecular OH···F HB appears as a driving force in guiding the conformational preferences of α-fluoro-*o*-cresols. The case of di- and trifluoro-*o*-cresols is of particular interest. Indeed, three-centre IMHB interactions appear as original features of highly populated conformations of these compounds and are preferred to two-centre IMHB interactions.

These conformational preferences lead to a drastic decrease of the OH group H-bond donating capacity upon monofluorination. Difluorination induces distinct effects: the fluorine electronwithdrawing effect compensates the influence of the IMHB, the H-bond acidity of α,α-difluoro-*o*-cresol being equal to that of *o*-cresol. In the case of methyl perfluorination, the fluorine electronwithdrawing effect dominates and a H-bond acidity increase is observed. If the intrinsic H-bond acidity of phenols remains stronger than benzyl alcohols, their respective fluorination reveals a modulation of this important physicochemical property which follows a completely opposite order.[26] This modulation is actually closer to the variations previously observed in the case of cyclic fluorohydrins.[21]

Therefore, this study reports new qualitative and quantitative features of OH···F IM H-bonding in α-fluoro-*o*-cresols and its impact on the hydroxyl group ability to behave as hydrogen-bond donor with an external acceptor. These findings will be of interest in the various fields where intermolecular hydrogen bonding are key interactions, for example in protein-ligand binding and in catalyst ligand design. Hence, the prospect of tuning the hydrogen-bond donating capacity of Ar-OH containing bioactive ligands will be particularly relevant for the design of drugs and probes in medicinal chemistry and chemical biology. The original findings described in this work therefore open up new opportunities for the optimisation of compounds through fluorination.

Acknowledgements

The Agence Nationale de la Recherche (ANR), through the ANR JCJC "ProOFE" grant (ANR-13-JS08–0007-01), and the Engineering and Physical Sciences Research Council (EPSRC), grant EP/K016938/1, are gratefully acknowledged for their financial support. The current work was granted access to the HPC resources of [CCRT/CINES/IDRIS] under the allocation c2014085117 made by GENCI (Grand Equipement National de Calcul Intensif) and HPC resources from ArronaxPlus (grant ANR-11-EQPX-0004 funded by the ANR). We thank the CCIPL (Centre de Calcul Intensif des Pays de la Loire) for grants of computer time.

Notes and references

1. M. Hird, *Chem. Soc. Rev.*, 2007, **36**, 2070.
2. J.-M. Vincent, *Chem. Commun.*, 2012, **48**, 11382.
3. E. P. Gillis, K. J. Eastman, M. D. Hill, D. J. Donnelly and N. A. Meanwell, *J. Med. Chem.*, 2015, **58**, 8315.
4. S. Purser, P. R. Moore, S. Swallow and V. Gouverneur, *Chem. Soc. Rev.*, 2008, **37**, 320.
5. D. O'Hagan, *J. Fluorine Chem.*, 2010, **131**, 1071.
6. J. Wang, M. Sanchez-Rosello, J. L. Acena, C. del Pozo, A. E. Sorochinsky, S. Fustero, V. A. Soloshonok and H. Liu, *Chem. Rev.*, 2014, **114**, 2432.
7. R. Berger, G. Resnati, P. Metrangolo, E. Weber and J. Hulliger, *Chem. Soc. Rev.*, 2011, **40**, 3496.
8. D. Chopra and T. N. G. Row, *CrystEngComm*, 2011, **13**, 2175.
9. P. Jeschke, *Pest Management Science*, 2010, **66**, 10.
10. T. Fujiwara and D. O'Hagan, *J. Fluorine Chem.*, 2014, **167**, 16.
11. P. A. Champagne, J. Desroches and J.-F. Paquin, *Synthesis*, 2015, **47**, 306.
12. H.-J. Schneider, *Chem. Sci.*, 2012, **3**, 1381.
13. D. O'Hagan, *Chem. Soc. Rev.*, 2008, **37**, 308.
14. J. D. Dunitz and R. Taylor, *Chem. Eur. J.*, 1997, **3**, 89.
15. J. A. K. Howard, V. J. Hoy, D. O'Hagan and G. T. Smith, *Tetrahedron*, 1996, **52**, 12613.
16. W. Adcock, J. Graton, C. Laurence, M. Lucon and N. Trout, *J. Phys. Org. Chem.*, 2005, **18**, 227.
17. C. Ouvrard, M. Berthelot and C. Laurence, *J. Phys. Org. Chem.*, 2001, **14**, 804.
18. C. Ouvrard, M. Berthelot and C. Laurence, *J. Chem. Soc., Perkin Trans. 2*, 1999, 1357.
19. C. Dalvit, C. Invernizzi and A. Vulpetti, *Chem. Eur. J.*, 2014, **20**, 11058.
20. M. Heger, T. Scharge and M. A. Suhm, *Phys. Chem. Chem. Phys.*, 2013, **15**, 16065.
21. J. Graton, Z. Wang, A.-M. Brossard, D. Goncalves Monteiro, J.-Y. Le Questel and B. Linclau, *Angew. Chem., Int. Ed.*, 2012, **51**, 6176.
22. B. Bernet and A. Vasella, *Helv. Chim. Acta*, 2007, **90**, 1874.
23. H. Takemura, R. Ueda and T. Iwanaga, *J. Fluorine Chem.*, 2009, **130**, 684.
24. K. Nakai, Y. Takagi and T. Tsuchiya, *Carbohydr. Res.*, 1999, **316**, 47.
25. B. Linclau, F. Peron, E. Bogdan, N. Wells, Z. Wang, G. Compain, C. Q. Fontenelle, N. Galland, J.-Y. Le Questel and J. Graton, *Chem. Eur. J.*, 2015, **21**, 17808.
26. E. Bogdan, G. Compain, L. Mtashobya, J.-Y. Le Questel, F. Besseau, N. Galland, B. Linclau and J. Graton, *Chem. Eur. J.*, 2015, **21**, 11462.
27. J. Graton, F. Besseau, A.-M. Brossard, E. Charpentier, A. Deroche and J.-Y. Le Questel, *J. Phys. Chem. A*, 2013, **117**, 13184.
28. M. H. Abraham, P. L. Grellier, D. V. Prior, P. P. Duce, J. J. Morris and P. J. Taylor, *J. Chem. Soc., Perkin Trans. 2*, 1989, 699.
29. R. F. W. Bader, *Chem. Rev.*, 1991, **91**, 893.
30. R. F. W. Bader, *Atoms in Molecules: A Quantum Theory*, Clarendon, Oxford, 1994.

31. E. R. Johnson, S. Keinan, P. Mori-Sanchez, J. Contreras-Garcia, A. J. Cohen and W. Yang, *J. Am. Chem. Soc.*, 2010, **132**, 6498.
32. F. Weinhold and C. Landis, R, *Valency and Bonding. A Natural Bond Orbital Donor-Acceptor Perspective.*, Cambridge University Press, Cambridge, 2005.
33. P. W. Kenny, *J. Chem. Inf. Model.*, 2009, **49**, 1234.
34. M. J. Frisch, G. W. Trucks, H. B. Schlegel, G. E. Scuseria, M. A. Robb, J. R. Cheeseman, G. Scalmani, V. Barone, B. Mennucci, G. A. Petersson, H. Nakatsuji, M. Caricato, X. Li, H. P. Hratchian, A. F. Izmaylov, J. Bloino, G. Zheng, J. L. Sonnenberg, M. Hada, M. Ehara, K. Toyota, R. Fukuda, J. Hasegawa, M. Ishida, T. Nakajima, Y. Honda, O. Kitao, H. Nakai, T. Vreven, J. A. Montgomery Jr., J. E. Peralta, F. Ogliaro, M. J. Bearpark, J. Heyd, E. N. Brothers, K. N. Kudin, V. N. Staroverov, R. Kobayashi, J. Normand, K. Raghavachari, A. P. Rendell, J. C. Burant, S. S. Iyengar, J. Tomasi, M. Cossi, N. Rega, N. J. Millam, M. Klene, J. E. Knox, J. B. Cross, V. Bakken, C. Adamo, J. Jaramillo, R. Gomperts, R. E. Stratmann, O. Yazyev, A. J. Austin, R. Cammi, C. Pomelli, J. W. Ochterski, R. L. Martin, K. Morokuma, V. G. Zakrzewski, G. A. Voth, P. Salvador, J. J. Dannenberg, S. Dapprich, A. D. Daniels, Ö. Farkas, J. B. Foresman, J. V. Ortiz, J. Cioslowski and D. J. Fox, *Gaussian 09*, (2009) Gaussian, Inc., Wallingford, CT, USA.
35. F. W. Biegler-Koenig, J. Schonbohm and D. Bayles, *J. Comput. Chem.*, 2001, **22**, 545.
36. E. Espinosa, C. Lecomte and E. Molins, *Chem. Phys. Lett.*, 1999, **300**, 745.
37. Y. A. Abramov, *Acta Cryst. A*, 1997, **A53**, 264.
38. E. Espinosa, I. Alkorta, I. Rozas, J. Elguero and E. Molins, *Chem. Phys. Lett.*, 2001, **336**, 457.
39. E. Espinosa, E. Molins and C. Lecomte, *Chem. Phys. Lett.*, 1998, **285**, 170.
40. J. Contreras-Garcia, E. R. Johnson, S. Keinan, R. Chaudret, J.-P. Piquemal, D. N. Beratan and W. Yang, *J. Chem. Theory Comput.*, 2011, **7**, 625.
41. H.-G. Korth, M. I. de Heer and P. Mulder, *J. Phys. Chem. A*, 2002, **106**, 8779.
42. A. Bondi, *J. Phys. Chem.*, 1964, **68**, 441.
43. S. J. Knak Jensen, J. C. Vank, T. H. Tang and I. G. Csizmadia, *Chem. Phys. Lett.*, 2000, **321**, 126.
44. A. Kovacs and I. Hargittai, *J. Phys. Chem. A*, 1998, **102**, 3415.
45. K. V. Hansen and T. Pedersen, *J. Mol. Struct.*, 1983, **97**, 311.
46. A. Kovacs, I. Kolossvary, G. I. Csonka and I. Hargittai, *J. Comput. Chem.*, 1996, **17**, 1804.
47. A. Dey and G. N. Patwari, *J. Phys. Chem. A*, 2012, **116**, 6996.
48. A. T. Ayoub, J. Tuszynski and M. Klobukowski, *Theor. Chem. Acc.*, 2014, **133**, 1.
49. U. Koch and P. L. A. Popelier, *J. Phys. Chem.*, 1995, **99**, 9747.
50. S. Shapiro, A. Bader and S. J. K. Jensen, *J. Mol. Struct. THEOCHEM*, 2004, **711**, 1.
51. A. Otero-de-la-Roza, E. R. Johnson and J. Contreras-Garcia, *Phys. Chem. Chem. Phys.*, 2012, **14**, 12165.
52. S. R. Hanson, L. J. Whalen and C.-H. Wong, *Bioorg. Med. Chem.*, 2006, **14**, 8386.
53. V. Ahmed, Y. Liu and S. D. Taylor, *ChemBioChem*, 2009, **10**, 1457.